Vehicle Driveability: Dynamic Analysis of Powertrain System Components

Vehicle Driveability: Dynamic Analysis of Powertrain System Components

Luca Castellazzi, Andrea Tonoli, Nicola Amati, Alessandro Piu, Enrico Galliera

CITATION: Castellazzi, L., Tonoli, A., Amati, N., Piu, A. et al., "Vehicle Driveability: Dynamic Analysis of Powertrain System Components," SAE Technical Paper 2016-01-1124, 2016, doi:10.4271/2016-01-1124.

Abstract

The term driveability describes the driver's complex subjective perception of the interactions with the vehicle. One of them is associated to longitudinal acceleration aspects. A relevant contribution to the driveability optimization process is, nowadays, realized by means of track tests during which a considerable amount of driveline parameters are tuned in order to obtain a good compromise of longitudinal acceleration response. Unfortunately, this process is carried out at a development stage when a design iteration becomes too expensive. In addition, the actual trend of downsizing and supercharging the engines leads to higher vibrations that are transmitted to the vehicle. A large effort is therefore dedicated to develop, test and implement ignition strategies addressed to minimize the torque irregularities. Such strategies could penalize the engine maximum performance, efficiency and emissions. The introduction of the dual mass flywheel is beneficial to this end. Nevertheless, its role on the vehicle driveability, as well as that of other driveline components, is not yet so clear. The aim of the present work is to establish which are the main driveline components affecting the filtering behavior of the transmission and how their parameters can be tuned in order to improve the vehicle ability to respond to driver's different demands without negative impact on his comfort. A complete nonlinear coupled torsional and longitudinal vehicle dynamic model is proposed to this end. The model is validated both in time and frequency domain and allows linearization of its nonlinear components.

Introduction

In the latest years, Noise, Vibrations and Harshness context for passenger cars has increased its importance becoming a crucial parameter for their competitiveness and markeatability. The term *driveability* describes the complex interactions between the driver and the vehicle regarding longitudinal acceleration aspects in terms of vibration transmissibility and fast response to driver inputs.

Today, track tests still play an important role in the overall driveability process optimization. The considerable amount of powertrain parameters that can be tuned (stiffness, damping of components) contribute to obtain optimal driveability metrics (kicks, jerks, overshoots) that should be translated into objective evaluations [1, 2, 3]. This needs long calibration time to find an acceptable compromise. In addition, this optimization process has the drawback to be carried out at a development stage in which a design iteration is very expensive.

Adequate mathematical models to be used at preliminary design stage to fix the main driveline component parameters are therefore extremely useful. Similar models are useful also at following design stages, before prototype construction, for engine control strategies calibrations. The literature on the subject is summarized here below.

Couderc et al. [4] presented a work about the prediction of dynamic behavior of drivelines including idle and drive gear rattle by means of a lumped parameter model including a complete driveline and the chassis longitudinal degrees of freedom. Model linearization allows frequency domain analysis. Capitani et al. [5] underlined that the range 1 – 10 Hz is the one that should be investigated in order to achieve information on driveability. In particular, analyzing the longitudinal acceleration spectrum, one resonance occurs at about 4 Hz and another at twice the first. Sorniotti [6] developed different driveline models of different complexity. The simplest includes only the half shafts compliance, the most complex includes the driveline dynamics in addition to chassis dynamics in terms of sprung mass and engine mounts degrees of freedom. A significant coupling between sprung and unsprung mass and between engine and gearbox has been evidenced.

Although a lot of work has been dedicated to the powertrain modeling and to the experimental validation of mathematical models for driveability analysis, there seems to be a little consideration on the effects of dual mass flywheel (DMFW) and engine suspensions on this subject. DMFW exploits a low frequency resonance to filter out the vibrations coming from the internal combustion engine and that can be transmitted to the driver. In addition to DMFW, engine suspension and unsprung masses suspensions can also contribute to vibrations attenuation.

The aim of this work is to study the influence of different powertrain components able to improve the vehicle driveability, and to understand which of the design parameters should be modified in order to improve the vehicle ability to respond to driver's different demands without negative impacts on his comfort.

The model at the base of the analysis is validated both in time and frequency domain and the linearization of its nonlinear components (i. e. dual mass flywheel, clutch and tire), allows to perform sensitivity analysis based on a modal energy approach.

Vehicle dynamic model

The aim of the mathematical model presented in this section is to reproduce both the torsional dynamics of the powertrain, and the

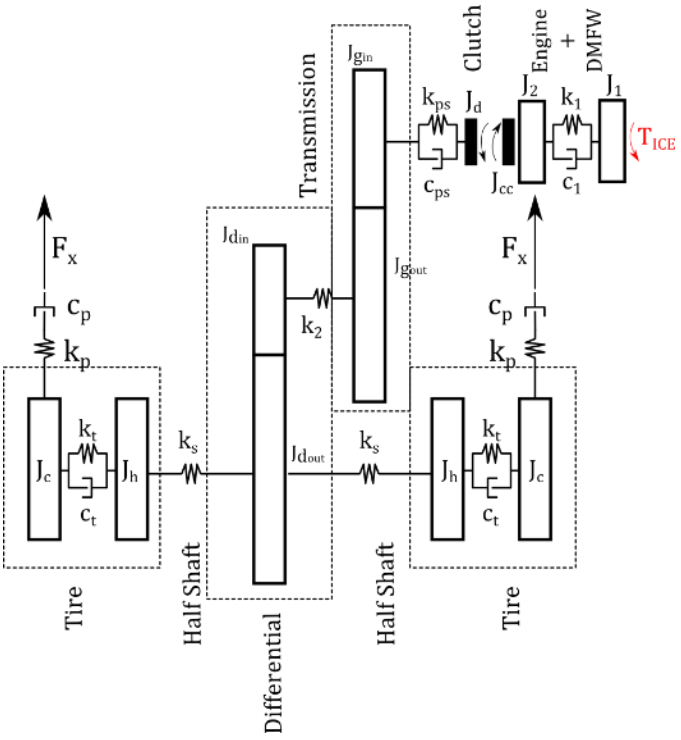

Figure 1. Model of rotating components.

longitudinal dynamics of the vehicle. The engine mounts and the longitudinal compliances of unsprung masses are included too. The inputs to the model are the internal combustion engine torque (T_{ICE}, depurated from belt drive system losses) and the external forces acting on the vehicle (F_{ext}). The linear part of the system is written in terms of state matrices. The nonlinear effects are included by means of external generalized forces that are computed starting from the relevant speeds or displacements. For example, the angular displacement and speed difference across the DMFW are used to compute the DMFW nonlinear spring, viscous damping and dry friction torques. They are fed back into the linear block. In the following, a description of the model is presented.

Figure 1 shows the model of the rotating parts. Engine and primary DMFW inertia are merged in a unique flywheel (J_1), secondary DMFW inertia and clutch cover are merged in flywheel J_2. k_1 is the nonlinear DMFW stiffness, c_1 is its viscous damping. Coulombian friction $T_{\mathrm{DMFW,C}}$ is modeled as:

$$T_{\mathrm{DMFW,C}} = C \cdot \tanh\left(\frac{\Delta\omega}{\omega_{\mathrm{ref,1}}}\right) \tag{1}$$

where $\Delta\omega$ is the relative speed between flywheels J_1 and J_2. Parameters $\omega_{\mathrm{ref,1}}$ and C have been experimentally identified from hysteresis cycles of DMFW. J_{d} is the clutch disc inertia, k_{ps} and c_{ps} are the clutch nonlinear stiffness and viscous damping respectively. Clutch torque is modeled as:

$$T_{\mathrm{c}} = nfFr_{\mathrm{m}} \cdot f(\Delta\omega) \tag{2}$$

where $f(\Delta\omega)$ is a nonlinear friction function, n is the number of surfaces in contact, f is the friction coefficient between the friction surfaces, F is the axial load and r_{m} is the mean radius. The inertia effect of the gearbox and of the differential is taken into account by means of

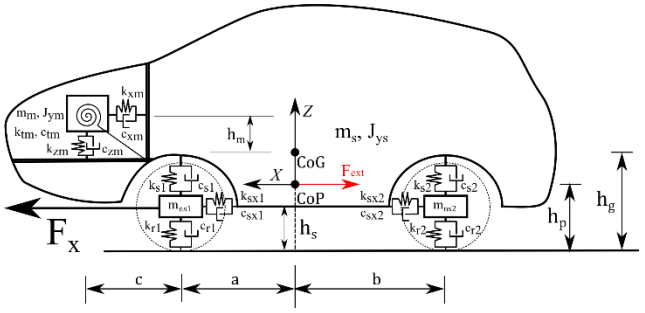

Figure 2. Longitudinal and vertical vehicle dynamics of the model.

flywheels $J_{\mathrm{gin}}, J_{\mathrm{gout}}, J_{\mathrm{din}}, J_{\mathrm{dout}}$. The terms k_2 and k_{s} indicate the torsional stiffness of the transmission shaft and of the half shafts while flywheels J_{h} and J_{c} simulate the wheel hub and tire rim respectively. Parameters k_t and c_t are the torsional stiffness and damping of the tire (sidewalls). A relaxation length model for the tire ground contact has been taken into account to couple the torsional and longitudinal dynamics. As shown in [7], the model considers a spring and a damper in series with variable coefficients k_{p} and c_{p}:

$$k_{\mathrm{p}} = \frac{BCD \cdot F_{\mathrm{z}}}{a_{\mathrm{w}}}; c_{\mathrm{p}} = \frac{BCD \cdot F_{\mathrm{z}}}{V} \tag{3}$$

where F_{z} is the normal load that takes into account for the longitudinal load transfer, BCD is the slope of the $\mu_x - \sigma$ curve, a_{w} is the half length of the contact patch and V is the vehicle speed.

Figure 2 shows the scheme of the vertical and longitudinal dynamics of the model. The vehicle body has mass m_{s}, moment of inertia J_{ys}. The pitch motion is about the pitch center CoP. Front and rear unsprung masses $m_{\mathrm{ns1}}$and m_{ns2} have vertical and longitudinal degrees of freedom. $k_{\mathrm{r1}}, c_{\mathrm{r1}}$ and $k_{\mathrm{r2}}, c_{\mathrm{r2}}$ are the vertical stiffness and damping of front and rear tire, $k_{\mathrm{sx1}}, c_{\mathrm{sx1}}$ and $k_{\mathrm{sx2}}, c_{\mathrm{sx2}}$ are the longitudinal stiffness and damping of front and rear unsprung masses. Suspensions are modeled with springs and dampers $k_{\mathrm{s1}}, c_{\mathrm{s1}}$ for the front and $k_{\mathrm{s2}}, c_{\mathrm{s2}}$ for the rear.

The engine and powertrain block is modeled with its mass and polar moment of inertia $m_{\mathrm{m}}$and J_{ym}. Engine mounts are modeled by means of springs and dampers $k_{\mathrm{xm}}, k_{\mathrm{zm}}, k_{\mathrm{tm}}$ and $c_{\mathrm{xm}}, c_{\mathrm{zm}}, c_{\mathrm{tm}}$ for longitudinal, vertical and torsional motion respectively.

Appendix 1 reports the nonlinear characteristics of the DMFW and clutch stiffness. They are implemented as look up tables.

The model has been implemented in MATLAB/Simulink environment.

Time and frequency domain simulations and validations

The aim of time and frequency domain validations is to understand if the model is robust enough to reproduce the desired phenomena in the relevant frequency range for driveability analysis (up to about 20 Hz). To this end, numerical longitudinal acceleration is then compared with the experimental one. Two numerical results are obtained. The first one, called 'linearized', is obtained linearizing the DMFW and clutch stiffness characteristics on their local slopes, and choosing a vertical

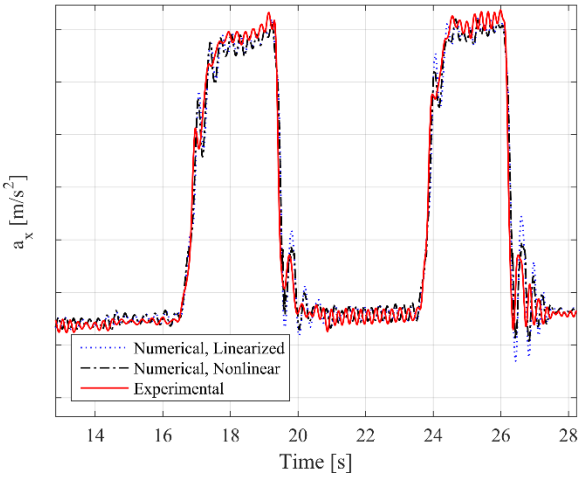

Figure 3. Vehicle longitudinal acceleration comparison between numerical and experimental results during a tip in/tip out maneuver in 2nd gear

load and a vehicle speed to linearize the tire. Appendix 1 shows the area of linearization of the different components. The second one, called 'nonlinear', takes into account all the non linearities present in the system. Experimental longitudinal acceleration is acquired by means of AVL® Data Acquisition System using a 3 – axis accelerometer ASC 5521with 0 – 5 V of Voltage measuring range and a sampling frequency of 100 Hz. This accelerometer is rigidly fixed to the vehicle body in a point close to the vehicle center of gravity (seat rail).

Figure 3 shows a comparison between numerical and experimental vehicle longitudinal accelerations during a tip in maneuver. As in the following Figs. 4 and 5, y – axis ticks are omitted for confidentiality reasons. The nonlinear model shows good fit both in the tip in and in the tip out phases. The much less damped response of the linearized model is justified by the fact that most of the dissipation in the system is due to the dry friction in the DMFW and clutch. These dissipations are modeled only in the nonlinear part of the model.

Figure 4 shows numerical and experimental longitudinal accelerations during an engine motoring phase. The strong oscillations between 44 and 46 s occur at a frequency of about 4 – 5 Hz. As it will be shown in the next section, this is the torsional natural frequency of the DMFW.

Figure 5 shows a good correlation between numerical and experimental acceleration during a gearshift maneuver.

Time domain simulations are useful as a first stage of the model validation. Nevertheless, a validation in the frequency domain is also performed considering the frequency response function (FRF) between the engine torque and the longitudinal acceleration.

Time domain signals during tip in/tip out maneuvers have been used to compute such frequency response function. As shown in Figure 6, the good match between numerical and experimental results up to about 10 – 15 Hz demonstrates the ability of the model to reproduce the most important frequency contributions of the signals from the driveability point of view.

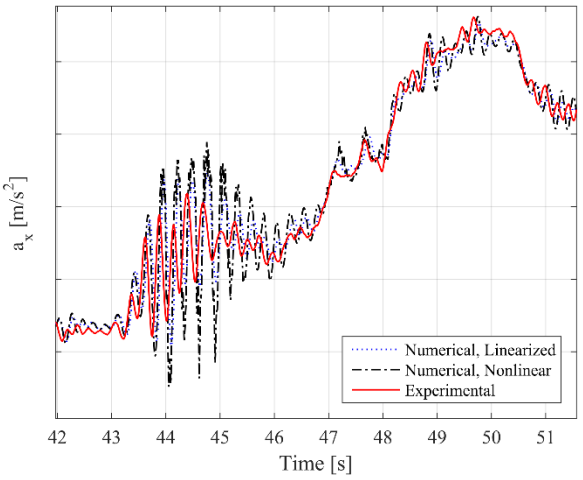

Figure 4. Vehicle longitudinal acceleration comparison between numerical and experimental results during a motoring maneuver in 2nd gear.

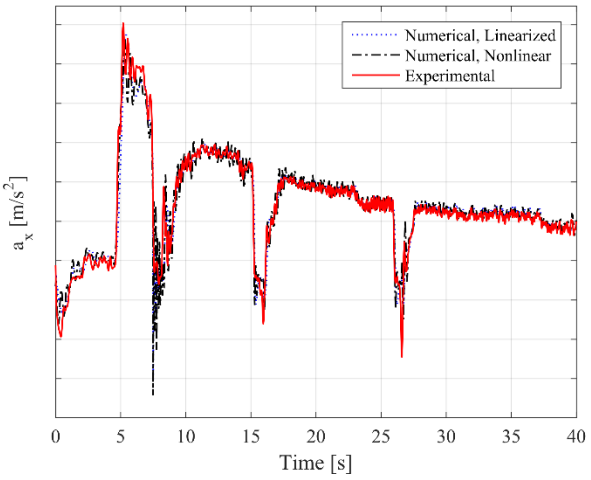

Figure 5. Vehicle longitudinal acceleration comparison between numerical and experimental results during an upshift maneuver.

The frequency response function shows a resonance at 5 Hz, followed by an attenuation range. Modal and energy analysis will be performed in the following to understand which powertrain components are mostly excited at each natural frequency. Sensitivity analysis will then show how much a natural mode is influenced by the variation of different system parameters.

Modal, energy and sensitivity analysis

One of the most interesting characteristic of a powertrain system is the *engine to driver* dynamic behavior. As already stated, the longitudinal acceleration is an important variable for the driveability judgment since it is directly correlated to driving comfort. An oscillatory and non-smooth behavior of the longitudinal acceleration is mainly caused by the harmonic contributions of the engine torque. Therefore in this context, the powertrain can be analyzed in terms of its ability to filter out the vibrations transmitted to the driver.

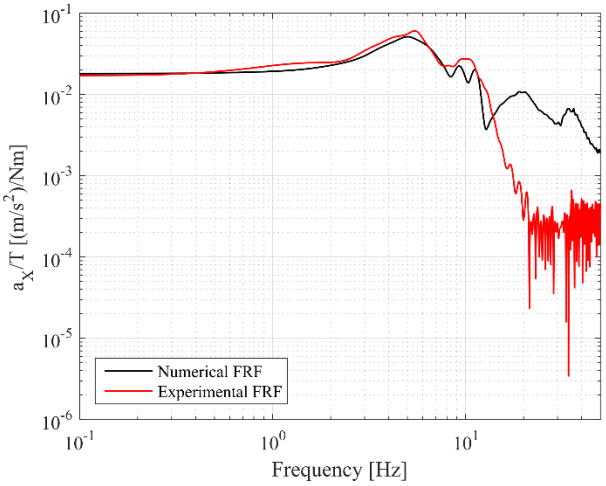

Figure 6. Comparison between numerical and experimental frequency response functions for the linearized configuration.

Modal analysis is then performed on the linearized system in order to understand which are its natural frequencies. Then, modal energy is computed to investigate the sensitivity of the system to different design parameters.

Modal and energy analysis

Natural frequencies of the system have been computed as the eigenvalues of the linearized system state matrix for different engaged gears. Figure 7 shows how the engaged gear affects the variation of each natural frequency of the system. Some modes ($1^{st}, 2^{nd}, 4^{th}, 8^{th}, 10^{th}$) are little or even not affected by the gear variation because they are related to unsprung mass and other components not belonging to the powertrain. Instead, other modes like the 3^{rd}, 6^{th}, 9^{th} and the 11^{th} are more influenced, with variations from 10 to 35 % (with respect to the natural frequencies of the first gear). This underlines how some modes have high influence on the dynamic behavior of the system, so that their natural frequency values change with the gear variation.

This kind of analysis does not allow to understand to which powertrain component each natural frequency is associated. Energy analysis rather than mode shapes analysis, is a powerful tool that allows to find which component stores most of the kinetic and potential energy at each natural mode.

A matrix of potential energies $[U] \in \mathbb{R}^{ixj}$ has been computed. Each term is expressed as:

$$u_{ij} = \frac{\frac{1}{2}k_i\left(\psi_{i,j} - \psi_{i+1,j}\right)^2}{\frac{1}{2}\{\psi\}_j^{\mathrm{T}}[K]\{\psi\}_j} \tag{4}$$

where $[K]$ is the stiffness matrix of the linearized system, $\{\psi\}_j$ is the eigenvector associated to the j – th mode and k_i is the i – th stiffness of the system.

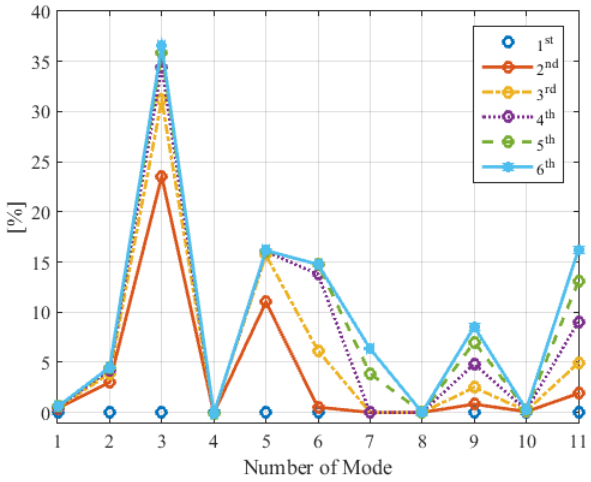

Figure 7. Variation of the first 11 natural frequencies of the system as a function of the different engaged gears. The variation is expressed as the increment percentage of the i^{th} natural frequency with a certain gear engaged with respect to the same one in first gear.

Figure 8 shows the modal potential energy contribution of the 15 springs of the system for the first 11 modes, both in 2^{nd} and in 4^{th} gear (left and right respectively). It is possible to evidence 4 main mode clusters, highlighted with letters A, B, C and D. Cluster A is dominated by bounce and pitch chassis modes because the stiffness that are mostly involved are the suspensions ones. Cluster B is dominated by the DMFW stiffness, but its influence on the same mode (3^{rd}) changes with respect to the engaged gear (~50% in 2^{nd} gear, ~85% in 4^{th} gear).

Cluster C is dominated by the engine suspension dynamics with longitudinal, vertical and torsional motion of the powertrain block with respect to the chassis body. Again, the influence of stiffness k_{xm} , k_{zm} and k_{tm} on the same mode changes with respect to the engaged gear. This highlights how the filtering components of the transmission strongly affect the driving dynamics at different vehicle working conditions. Cluster D is dominated by the motions related to the longitudinal and vertical degrees of freedom of the unsprung masses. Very small influence of the engaged gear is evidenced in this case.

Table 1 summarizes the first 11 natural frequencies of the system and the associated modes in 2^{nd} gear engaged.

The frequency response function between the engine torque (input) and the longitudinal acceleration (output) can be computed from the undamped linearized system. Figure 9 shows the influence of the engaged gear on such frequency response function. For low frequencies the response is flat and dominated by the equivalent translating inertia:

$$G = \frac{i_g \cdot i_d}{R \cdot m_{at}} \tag{5}$$

where G is the low frequency gain, i_g and i_d are the transmission ratio of the gearbox and of the differential respectively, R is the effective tire rolling radius and m_{at} is the apparent or equivalent translating mass. A smaller transmission ratio, consistent with a higher engaged gear, realizes a smaller low frequency gain.

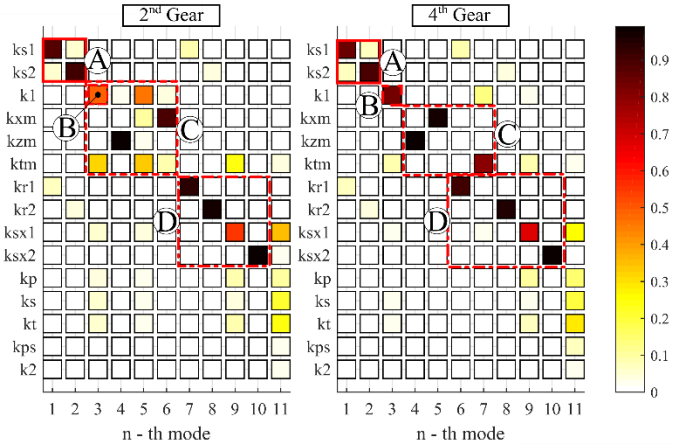

Figure 8. Modal energy contribution of different stiffness in modes 1 to 11, corresponding to a frequency range between 1 and 35 Hz for 2nd gear (left) and 4th gear (right).

Table 1. Summary of the first natural frequencies of the system and the associated modes with 2nd gear engaged.

Frequency [Hz]	Mode
1.1	Chassis/Body
1.3	Chassis/Body
5	DMFW and Torsional Engine Mount
8.5	Vertical Engine Mount
10	Torsional and Longitudinal Engine Mount
11	Longitudinal Engine Mount
13	Vertical Motion of Front Unsprung Mass
18	Vertical Motion of Rear Unsprung Mass
19	Torsional Engine Mount and Longitudinal Motion of Front Unsprung Mass
32	Longitudinal Motion of Rear Unsprung Mass
36	Half Shafts, Torsional Motion of Tire

The 4 main clusters are still evidenced, and it is possible to observe that for the mid - range frequencies (5 – 30 Hz), the resonance peaks move to different values if the engaged gear is higher, as shown in previous analysis (Figure 7 and 8).

A *low pass filter* trend can be evidenced, and what should be underlined is that a shifting to higher gear increases the cut off frequency (from 5 to 6 Hz, from 2nd to 4th gear) and leads to smaller attenuation.

Sensitivity analysis

Previous analysis showed how the powertrain dynamic characteristics change with respect to the engaged gear, and how this can affect the response of the system in terms of longitudinal acceleration relative to an input torque with a certain frequency content.

The powertrain can be seen as a low pass filter, and its first natural frequency (the one relative to the DMFW) affects the cut off (B cluster, Figures 8 and 9). In addition, other resonances such as those relative

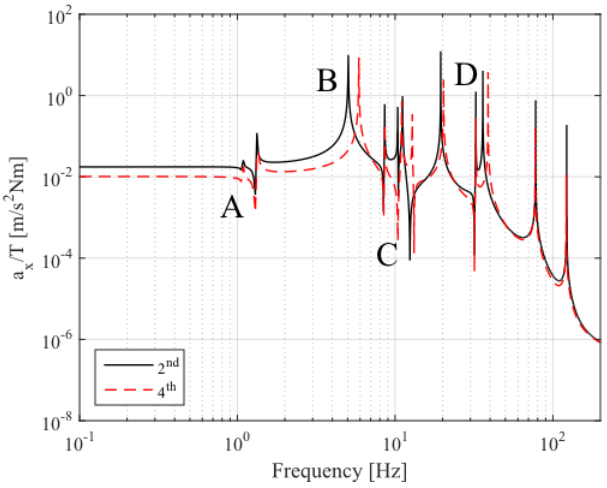

Figure 9. Frequency response function between input torque and output longitudinal acceleration of the undamped linearized system in 2nd and 4th gear.

to the engine mounts (C cluster) contribute significantly to the overall filtering behavior of the transmission system.

Therefore in the following, a parametric study is performed on the natural frequencies of the system, to understand how they change as a function of the dominant factors of B and C clusters, i.e. the DMFW and torsional engine mount stiffness.

Figure 10 shows the first 6 natural frequencies of the system in 2nd gear as a function of the individual variation of DMFW stiffness (k_1, continuous black) and torsional engine mount stiffness (k_{tm}, dashed red). Being the first two modes relative to bounce and pitch motion of the sprung mass, their natural frequencies remain constant in all the parameters range. By converse, as already evidenced in Figure 8, the third mode is strongly affected by the DMFW stiffness. It is interesting to note that this mode is also affected by the torsional engine mount stiffness, which produces a variation of the natural frequency comparable to that due to the DMFW stiffness.

The fourth mode is the one related to the vertical bounce of the engine block, and apart the non realistic case of large reduction (- 80%), it is weakly influenced by the variation of the two parameters under analysis.

Fifth and sixth modes are a sort of coupled modes. This is confirmed also by observing the plot of modal potential energies (Fig. 8, left) in which mode 5 and 6 are dominated both by k_{xm} and k_{tm} at the same time. Figure 10 shows that the sixth mode is not affected by DMFW stiffness up to almost + 20%. Conversely, fifth mode increases its natural frequency until the same amount of variation. After this threshold the behavior of the two modes is the opposite: fifth mode remains almost insensible to the variations, and sixth mode increases its natural frequency. The two natural frequencies never cross each other and a veering phenomenon is then evidenced.

For the case of 4th gear engaged, Figure 11 shows that DMFW variation affects the 3rd mode in addition to 6th and 7th ones, that show a coupled behavior (veering effect present at about 20% of DMFW stiffness variation).

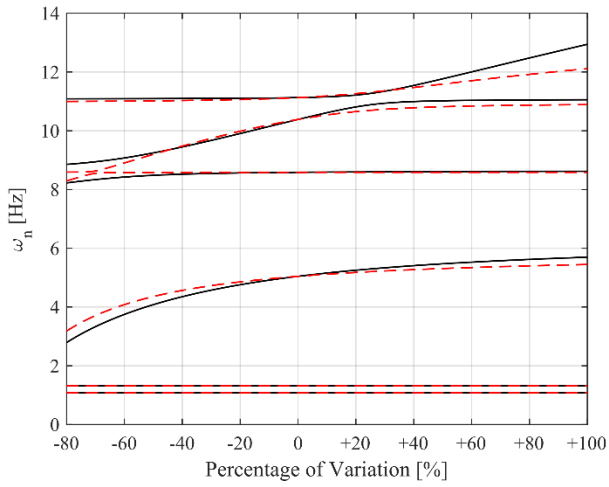

Figure 10. First 6 natural frequencies of the system as a function of the variation of the DMFW stiffness (continuous black) and of the torsional stiffness of the engine mounts (dotted red) for 2nd gear engaged.

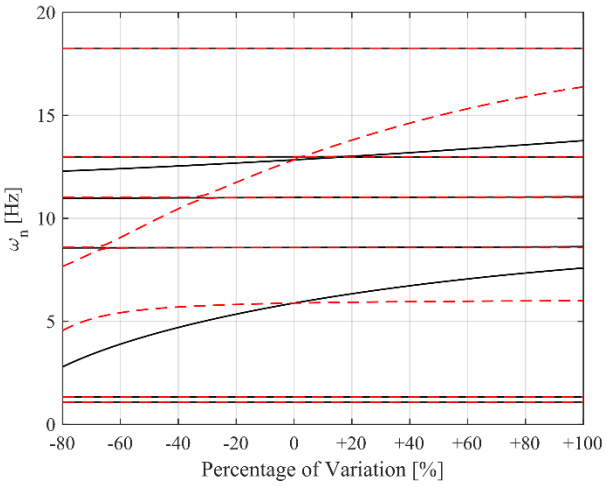

Figure 11. First 8 natural frequencies of the system as a function of the variation of the DMFW stiffness (continuous black) and of the torsional stiffness of the engine mounts (dotted red) for 4th gear engaged.

This could be noticed also looking to the modal energies diagram (Figure 8, right) in which it is showed that mode 7 is influenced both by $k_{tm}$and by k_1. k_{tm} variation causes a high level of coupling of the mid – range modes, creating three zones in which veering is present (~-70%, ~-30%, ~5%). This confirms the not negligible impact of the engine mounts torsional stiffness.

In addition to the study of the system natural frequency variation, another important quantity that should be analyzed is the amplitude of the frequency response. Figure 12 shows the frequency response function between the input torque and the output longitudinal acceleration of the damped system with the 2nd gear engaged. Three different values of the DMFW stiffness (nominal, half and twice) have been considered. The same has been done for the engine mount torsional stiffness (Fig. 13). The tire is linearized assuming a vehicle speed of 20 km/h.

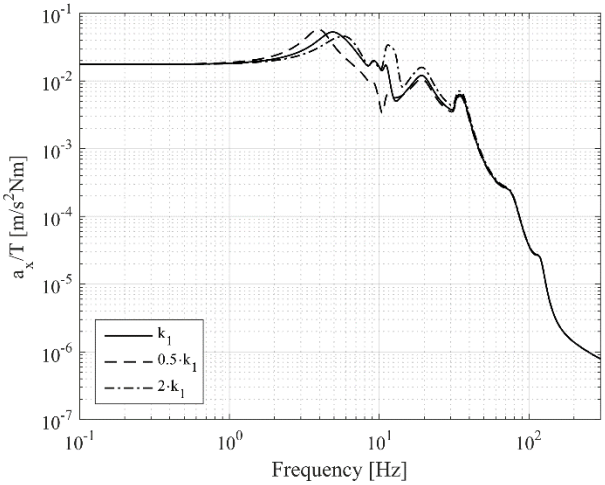

Figure 12. Frequency response function between input torque and output longitudinal acceleration in 2nd gear engaged considering a sensitivity on the

DMFW stiffness k_1: nominal value (continuous), half the nominal value (dashed), twice the nominal value (dashed dotted).

The resonance of the first two modes (chassis mode, ref. to Table 1) do not show any peak as they are completely damped out by the suspensions. The comparison of the two plots (Figs. 12 and 13) shows that the main effect of DMFW and engine mount stiffness is in the frequency range of cluster B and C modes (4 – 15 Hz). Reducing the stiffnesses lowers the first mode and improves the attenuation in the 4 – 15 Hz band. Increasing the stiffnesses above the nominal value, reduces the attenuation in same band and leads to larger amplitudes of the cluster C modes. Both parameters (DMFW and engine mount stiffnesses) seem to have a similar effect on the response, this suggests the need of a tradeoff between their values in order to obtain a good balance between filtering performance and avoiding excessive deflections during max torque transmission and starting phases.

High frequency modes (from 30 Hz on) do not show any variation, consistently with the fact that the DMFW is able to act only on a limited frequency range.

The sensitivity analysis showed how the powertrain dynamic behavior is influenced by different system parameters. In particular, the engine to driver dynamic behavior of the transmission and its ability to attenuate the vibrations, strongly depend on the design of the DMFW and engine mount stiffnesses.

Reducing the natural frequency of these modes allows improving filtering because the frequency response function $a_x(\omega)/T(\omega)$ starts to attenuate the output from lower frequencies. Additionally, the sensitivity analysis shows that the 3rd mode is influenced both by the DMFW and engine suspension stiffnesses in 2nd gear. In 4th gear, instead, this mode is influenced mainly by the DMFW stiffness while the engine suspension one has relatively low impact. This suggest that at design stage the 3rd mode (that can be defined as DMFW mode) should be tuned at higher gears where engine suspension is less effective. Once DMFW stiffness is fixed, engine mounts can be tuned in 1st or 2nd gears.

The sensitivity analysis in different driving conditions highlights the role played by the engaged gear on the transmissibility of engine torque irregularities to the longitudinal acceleration.

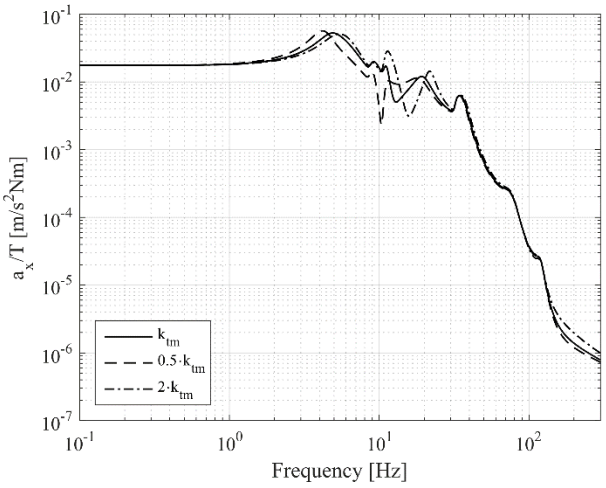

Figure 13. Frequency response function between input torque and output longitudinal acceleration in 2nd gear engaged considering a sensitivity on the DMFW stiffness k_{tm}: nominal value (continuous), half the nominal value (dashed), twice the nominal value (dashed dotted).

Conclusions

A dynamic model for vehicle driveability analysis has been presented. It has been validated by experimental data coming from a test campaign that covers a wide range of maneuvers. The model has been configured to have the linear part arranged in a subsystem interacting with an additional one implementing the nonlinear contributions. This was useful to use the linear subsystem (proper linearization points were identified) for modal and frequency response computations. The modal energy analyses highlighted the effects of the DMFW and engine mounts torsional stiffnesses on the mode shapes that are in the frequency range 4 – 15 Hz. The vibrational potential energy of the 3rd mode (4 ÷ 5 Hz) is mainly stored in the DMFW spring while that of the 5th one is mainly accumulated in the engine torsional stiffness term even if 4 main vibrational mode clusters can be identified. The 2nd and the 3rd clusters are mainly linked to the vibration motion of the powertrain and are affected by the engaged gear. The frequency response function between input torque and output longitudinal acceleration evidenced a low pass filter trend, characterizing the engine to driver vibrations transmissibility characteristics of the powertrain. The fundamental role is played by the dual mass flywheel because it determines the first torsional natural frequency affecting the cut off.

References

1. List, H. O., Schoeggl, P., “Objective Evaluation of Vehicle Driveability”, SAE Technical Paper 980204, 1998, doi: 10.4271/980204.
2. Dorey, R. and Holmes, C., "Vehicle Driveability - Its Characterisation and Measurement," SAE Technical Paper 1999-01-0949, 1999, doi: 10.4271/1999-01-0949.
3. Choi, Y.C., Song H.B., Lee J.H., Cho H.S., “An Experimental Study for Drivability Improvements in Vehicle Acceleration Mode”, Proceedings of the Institution of Mechanical Engineers, Part D: Journal of Automobile Engineering, Vol 217, No. 7, 2003, doi: 10.1243/095440703322115004
4. Couderc, P., Callenaere, J., Der Hagopian, J., Ferraris, G., Kassai, A., Borjesson, Y., Verdillon, L., Gaimard, S., “Vehicle Driveline Dynamic Behaviour: Experimentation and Simulation”, Journal of Sound and Vibration, Vol. 218, No. sv981808, 1998, doi: 10.1006/jsvi.1998.1808
5. Capitani, R., Delogu, M., Pilo, L., “Analysis of the influence of a vehicle's driveline dynamic behavior regarding the performance perception at low frequencies”, SAE Technical paper 2001 - 01 - 3333, 2001, doi: 10.4271/2001-01-3333.
6. Sorniotti, A., “Driveline Modeling, Experimental Validation and Evaluation of the Influence of the Different Parameter on the Overall System Dynamics”, SAE Technical Paper, 2008-01-0632, 2008, doi: 10.4271/2008-01-0632.
7. Pacejka, H., Besselink, I., “Tire and Vehicle Dynamics”, Third Edition, Elsevier, ISBN: 978-0-08-097016-5, 2012

Contact Information

Luca Castellazzi, Politecnico di Torino,

DIMEAS – Department of Mechanical and Aerospace Engineering,

LIM – Mechatronics Laboratory,

Corso Duca degli Abruzzi 24, 10129 Torino (Italy).

Phone: (+39) 011 090 6240.

Appendix 1 – DMFW and Clutch Stiffness Characteristics

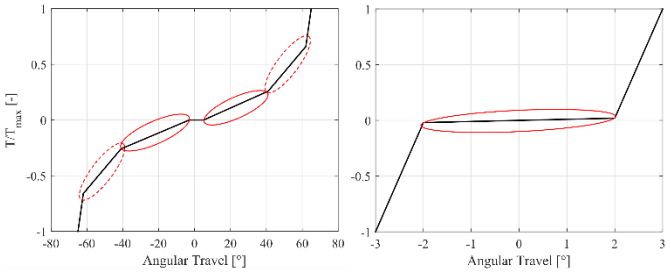

Figure 14. Dual mass flywheel (left) and clutch stiffness (right) characteristics. Different areas of linearization are showed (red circles).